Available online at www.eccomasproceedia.org
Eccomas Proceedia COMPDYN (2019) 2316-2331

ECCOMAS
Proceedia

COMPDYN 2019
7th ECCOMAS Thematic Conference on
Computational Methods in Structural Dynamics and Earthquake Engineering
M. Papadrakakis, M. Fragiadakis (eds.)
Crete, Greece, 24–26 June 2019

ENERGY DISSIPATION CAPACITY OF RC COLUMNS SUBJECTED TO UNIDIRECTIONAL AND BIDIRECTIONAL SEISMIC LOADING

D. Galé-Lamuela[1], J. Donaire-Avila[2], and D. Escolano-Margarit[3], G. González-Sanz[4] A. Benavent-Climent[5]

[1] Universidad Politécnica de Madrid, Department of Mechanical Engineering
José Gutiérrez Abascal, 2, 28006 Madrid, Spain
david.gale@upm.es

[2] University of Jaén, Department of Mechanical and Mining Engineering
Escuela Politécnica Superior de Linares Campus Científico Tecnológico de Linares Spain
jdonaire@ujaen.es

[3] Universidad Politécnica de Madrid, Department of Mechanical Engineering
José Gutiérrez Abascal, 2, 28006 Madrid, Spain
d.escolano@upm.es

[4] Universidad Politécnica de Madrid, Department of Mechanical Engineering
José Gutiérrez Abascal, 2, 28006 Madrid, Spain
guillermo.gonzalez.sanz@upm.es

[4] Universidad Politécnica de Madrid, Department of Mechanical Engineering
José Gutiérrez Abascal, 2, 28006 Madrid, Spain
amadeo.benavent@upm.es

Abstract

One of the gaps of knowledge for the application of the energy-based approach to conventional structures concerns the evaluation of the energy dissipation capacity of structural elements and systems. Addressing this issue calls for experimental data on structural members, structures or substructures subjected to realistic seismic loadings. The best source for such information is the dynamic shake table test. It can reproduce complex effects such as cumulative damage and rate-of-loading effects, that play an important role in the response of the structure. However this type of tests are very costly and time consuming. Therefore, it is necessary to complete the test information with numerical simulations. This paper provides information on the energy dissipation capacity of columns subjected to one and to two components of the seismic action. This information comes from shake table test conducted on RC waffle flat plate structures supported on isolated columns. The energy dissipated at the base of the columns until collapse is estimated applying different approaches.

Keywords: energy dissipation capacity, RC columns, shake table tests, unidirectional seismic loading, bidirectional seismic loading

ISSN:2623-3347
Peer-review under responsibility of the organizing committee of COMPDYN 2019.
doi: 10.7712/120119.7078.19108

1 INTRODUCTION

The most straightforward way to characterize the loading effect of earthquakes on structures is in terms of energy dissipation demand. In contrast to forces or displacements, which are vectors, energy is a scalar measure that can synthesize in a single value the complex 3D loading effects caused by earthquakes on structures [1]. Thus, comparing the energy dissipation demand with the energy dissipation capacity of the structure becomes the most rational way to evaluate structural safety, which in turn constitutes the basis of the energy-based approach. The energy dissipation demand at the global (overall structure) or local (structural members) level can be readily estimated from the total energy input by the earthquake. This estimation is facilitated by the fact that the energy input by an earthquake is a very stable quantity that depends almost exclusively on the mass and fundamental period of the structure, and it is scarcely affected by the viscous damping ratio, the post-yield hardening ratio, the degree of inelastic action or the number of degrees of freedom [2]. Past research on the energy-based approach focused on the energy dissipation demand side of the problem, addressing two aspects with different extent: (i) the estimation of the total amount of energy input by an earthquake, and (ii) its distribution among the structural components, that is the energy dissipation demand at the storey or structural member level. Most research effort has been devoted to the former while the later needs further development. In contrast to the energy dissipation demand, research on the energy dissipation capacity of structural elements and systems is almost inexistent and constitutes a fertile field for research.

Estimating the energy dissipation capacity of structural elements under seismic-type dynamic loadings is a cumbersome and challenging issue. One of the reasons for that is the path-dependency of the amount of energy that a structural element can dissipate until failure (i.e. the ultimate energy dissipation capacity) . That is, it is influenced by the distribution of the plastic cycles during the deformation history [3]. The number and amplitude of cycles of deformation imposed by earthquakes has a very random nature. They can hardly be converted into a sequence of closed cycles of constant amplitude, as counting methods such as the rain-flow or the range-pair methods do for histories with few reversals to failure. Dynamic shake tests of complete or partial structures that include the structural component under study, are the most realistic way to reproduce the response of a structural component subjected to a real earthquake. This kind of tests consider phenomena such as the variations of boundary conditions on the structural component within the structure (i.e. changes of the inflexion point in columns) or the simultaneous effects of bidirectional bending moments and axial forces. However, evaluating the energy dissipation capacity of the structural component from its results is cumbersome due to the limited information provided by the instrumentation. In addition shake table tests are expensive and time consuming, therefore it is necessary to complete the information provided by this type of test with numerical simulations.

This paper discuss several approaches to estimate the energy dissipation capacity of reinforced concrete (RC) column bases from unidirectional and bidirectional shake table tests conducted on waffle-flat plate structures subjected to one and two horizontal components of ground motion.

2 DESCRIPTION OF SHAKE TABLE TESTS

2.1 Prototype structure and test specimen

A prototype structure consisting of a three-story RC waffle-flat-plate system supported on isolated columns was designed to sustain gravity loads and lateral seismic loads prescribed in the

current Spanish Seismic Code NCSE-02. The depth of the slab was 0.35m with voids forming an orthogonal grid of ribs separated 0.83 m to each other. The plate had a solid head around the columns. Along the perimeter, the plate was surrounded by transverse beams of the same depth (0.35m). The loads considered were: 3.13 kN/m2 and 3.46 kN/m2 as dead loads for floors and roof; and 2 kN/m2 and 1 kN/m2 as live loads for floors and roof, respectively. The structure corresponded to an ordinary building located in Granada (Spain) on soil type C (180<vs,30<360, where $v_{s,30}$ is the average shear wave velocity in m/s). A behavior factor μ=2 was adopted to reduce the elastic response spectra, as prescribed by the NCSE-02 for flat-plate systems. The mechanical properties of materials were f_c=25 MPa for the concrete compressive strength and f_y=500 MPa for the yield strength of steel. A capacity design and ductile detailing was used for the columns to prevent shear failure before flexure failure, resulting in a design base shear force coefficient of 0.33.

From the prototype, a partial structural model consisting in three columns and one story and a half was isolated. The test specimen was defined from the partial structural model applying scale factors of λ_L=2/5 for length, λ_a=1 for acceleration and λ_σ=1 for stress. Other physical quantities were scaled to satisfy similitude requirements. Figure 1 shows the geometry and reinforcing details of the test specimen. The ratios of longitudinal reinforcement area, A_{sl} , to the gross section area, A_g, were A_{sl}/A_g=0.031 and A_{sl}/A_g=0.024 for the exterior and interior columns of the first floor, and A_{sl}/A_g=0.018 for all columns of the second floor. The volumetric ratio of shear reinforcement $\rho_{st} = V_{st}/V_{cc}$ was 0.03 for interior columns of the first floor and 0.02 for the rest. Where $V_{st}=nA_{st}l_s$ is the volume of the shear reinforcement (n, A_{st}, l_s are the number, cross-section area and length of the stirrups) and V_{cc} is the volume of concrete confined by the shear reinforcement. The waffle-flat plate was provided with an upper and lower base reinforcement consisting of a mesh of Ø6 bars separated 332 mm. Additional longitudinal rebars of Ø6 mm and Ø8 mm were located on the solid head of the plate around each column. A more detailed description of the prototype and test specimen can be found in references [4,5].

2.2 Test setup and instrumentation

A general view of the test setup and instrumentation is shown in Figure 2. The reacting mass and gravity loads were imposed through steel blocks attached at each floor (Figure 2) so as to satisfy similitude requirements. The instrumentation consisted of uniaxial accelerometers, displacement transducers and 472 strain gauges fixed to the longitudinal reinforcement. Strain gauges were located at column ends and in the critical regions of the solid heads of the plate around the columns. Figure 3 shows a detail of the position and number of strain gauges at the base of the exterior column (C1) that is the focus of this study. Two strain gauges, diametrically opposite each other and on the same cross section, were attached to each rebar. The average value of the two measurements was used as strain ε_{Sr} of the rebar.

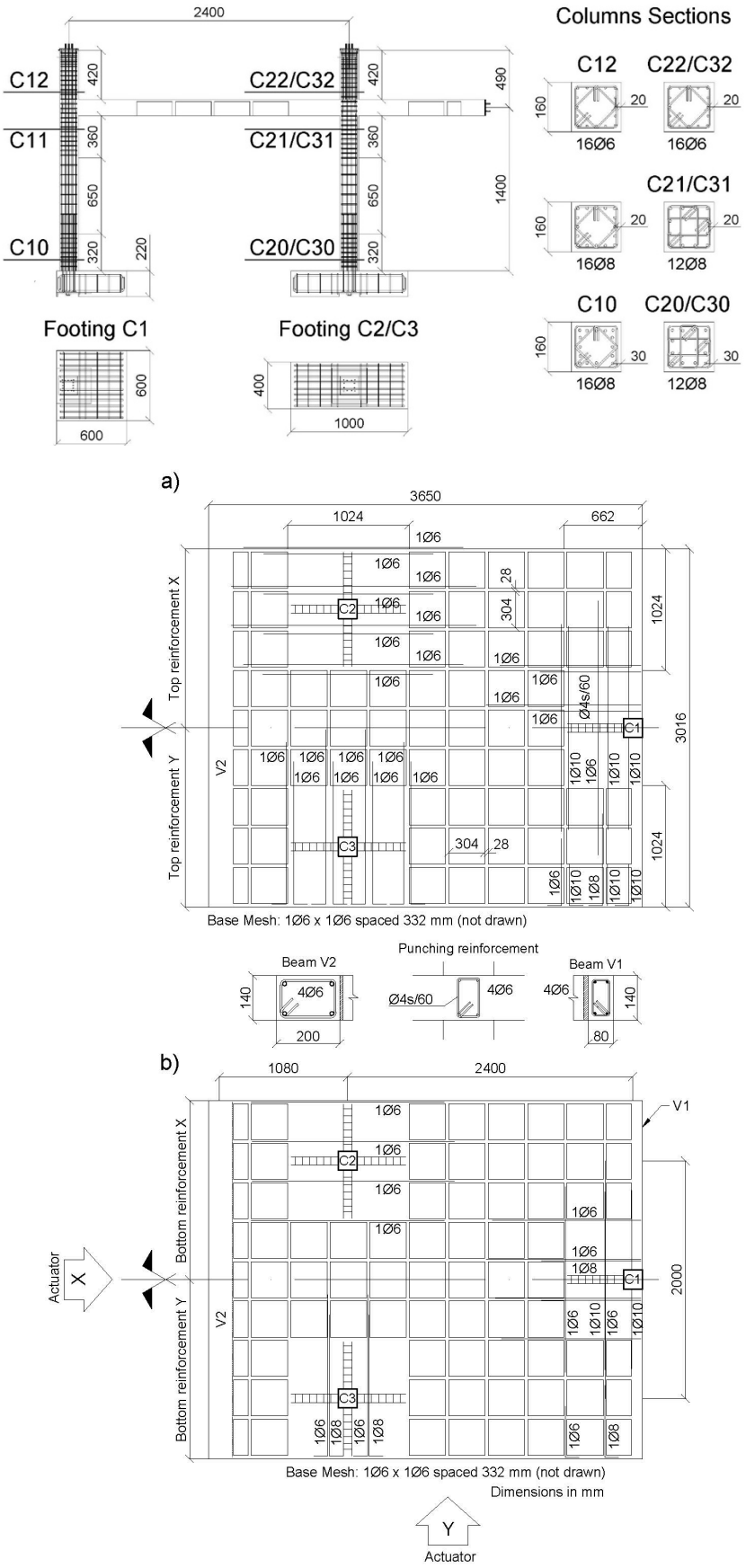

Figure 1: Test specimen

The displacement transducers measured in-plane translations, interstory drifts, and curvatures in columns and plate. The sampling rate of the data acquisition system was 600 Hz. Video cameras recorded the tests, and especially the movements at column bases.

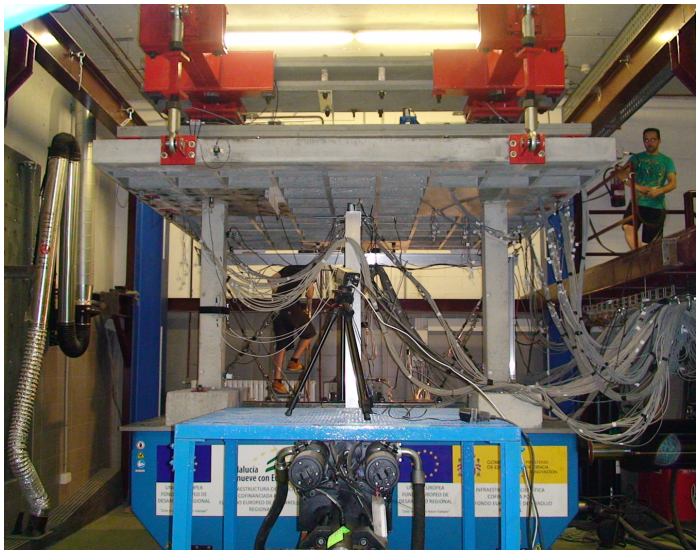

Figure 2: Test set-up and instrumentation

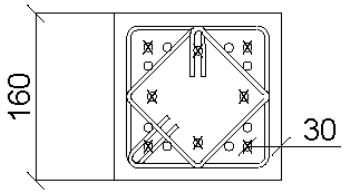

Figure 3: Position of strain gauges (×) at base of exterior column (C1)

2.3 Seismic tests

Two identical specimens with the geometry and reinforcement described in section 2.1 were built in the Laboratory of Structures of the University of Granada (Spain) in different periods of time. They will be referred to as BS and BS1 hereafter. Steel of the same batch was used for both specimens. The yield stress of longitudinal rebars of diameters 8 (Ø8) and 6mm (Ø6) were 525 and 543MPa respectively. The yield stress of the steel used for stirrups was 656MPa. The same concrete mix was used for both specimens with different casting dates. Compression tests conducted on samples from concrete casted in specimen BS resulted in compressive strengths of 39 MPa at 28 days and 43 MPa the day of the tests. For specimen BS1 in resulted in compressive strengths of 43 MPa at 28 days and 44 MPa the day of the tests.

Both specimens were subjected to dynamic tests using an MTS 3×3 m^2 shake table. In both cases, the horizontal components (NS and EW) of ground acceleration recorded at Calitri during the Campano Lucano (1980) earthquake were used. Specimen BS was subjected to the NS component of the ground motion (unidirectional loading), while specimen BS1 was subjected simultaneously to the two components, NS and EW, of the ground motion. The original acceleration records were scaled in time by the scaling factor $\lambda_t=(\lambda_L/\lambda_a)^{0.5}=0.63$. The original acceleration records were scaled also in amplitude to 100%, 200%, 300% and 350% in case of specimen BS, and to 35%, 50%, 100%, 200% and 300% in case of specimen BS1. Due to a

problem with the control system of the shaking table, the 200% test was repeated twice. The first attempt to apply the records scaled by 200% to specimen BS1 (referred to as test C200i hereafter) was interrupted at half of its original duration. The test was then repeated with the same amplitude (test C200) and completed successfully. The amount of energy input to the specimen by the failed test C200i was only one third of that input in the successful test C200. In the case of specimen BS subjected to unidirectional loading, the four seismic simulations will be referred to as C100, C200, C300 and C350 hereinafter and the corresponding peak ground accelerations, PGAs, were 0.16g, 0.31g, 0.47g and 0.55g, where g is the acceleration of gravity. In the case of specimen BS1, subjected to bidirectional loading, the PGA does not necessarily occur in the NS or EW direction and it was calculated as follows. Calling $GA_{NS}(t)$ and $GA_{EW}(t)$ the horizontal acceleration at instant t in the NS and EW directions, the acceleration at instant t in a direction forming a counterclockwise angle θ with EW-axis is $GA(t,\theta)=GA_{NS}(t)\sin\theta+GA_{EW}(t)\cos\theta$. The value of $GA(t,\theta)$ was calculated for different t and θ, and the maximum was taken as PGA. The PGAs obtained are 0.07g, 0.10g, 0.19g, 0.39g, 0.39g and 0.59g for the tests referred to herein as C35, C50, C100, C200i, C200 and C300 respectively.

3 ANALYSIS OF TEST RESULTS

For simplicity the following discussion will only focus on the response, in terms of energy dissipation capacity, of the exterior column C1 base. When necessary, reference will be done to the total amount of energy dissipated by the test specimen. A detailed description of the overall performance of the specimens can be found in references [4,5].

3.1 Overall performance of column bases

Specimen BS

During test C100 the strains in longitudinal bars at the column base remained below $0.75\varepsilon_y$. Early in test C200, a plastic hinge with ductile flexural yielding developed at the base of column C1, showing maximum strains of $1.13\varepsilon_y$. During test C300 cracks and concrete spalling was observed at column base, and the maximum strains of the longitudinal reinforcement reached $2.2\varepsilon_y$. During test C350 the base of column was heavy damaged, involving severe concrete crushing (see Figure 4) and strains up to $7.8\varepsilon_y$ were measured in the longitudinal reinforcement. Figure 4 shows the state of the base of column at the end of the tests.

Figure 4: Specimen BS. Final state of exterior column C1

Specimen BS1

At the end of tests C35 and C50 hairline flexural cracks were visible at column base. During these simulations, the maximum strains in longitudinal rebars reached $0.5\varepsilon_y$. Strains increased during simulation C100 reaching $5.1\varepsilon_y$. A visual inspection of the column base after tests C200i and C200 revealed concrete crushing and gauges attached to the longitudinal reinforcement measured strains up to $6.8\varepsilon_y$. Concrete spalling occurred during test C300, and the maximum strains in longitudinal rebars reached $7\varepsilon_y$.

Figure 5: Specimen BS1. Final state of exterior column C1

3.2 Procedure for evaluating the energy dissipated at column bases

The elastic strain energy stored, $W_{es,k}$, and the plastic strain energy dissipated, $W_{p,k}$, in a plastic hinge k located at a column base from instant t=0 to a given instant $t=t_t$ is the sum of the energy stored/dissipated by concrete, $W_{C,k}$, and by steel, $W_{S,k}$. The term "plastic hinge" refers to the region of the column end delimited by two parallel planes perpendicular to the longitudinal reinforcement and spaced a distance l_p. $W_{C,k}$ and $W_{S,}$ can be estimated as follows. The cross section of the plastic hinge, of depth h and width b, is divided in $N\times N$ fibers of depth h/N and width b/N. A material (steel or concrete) is assigned to each fiber, depending on the position of the rebars in the RC section. It is assumed that each fiber experiences the same strain along its length l_p. Based on these assumptions, the strain at any instant t of any fiber i of the cross section $\varepsilon_i(t)$, was estimated from the strains measured at the gauges adhered to the longitudinal rebars ε_{Si} (see Figure 3) applying two different approaches:

a) *Plane approximation*. A plane defined by the equation ($x=ay+bz+c$) was obtained at each time step using the method of least squares. The method minimizes the sum of the squared difference between the actual strain ε_{Si} measured by the strain gauge i located at coordinates (y_i, z_i) of the cross section, and the estimated value x_i on the plane. That is, the function to minimize is $E=\sum_{i=1}^{n}[\varepsilon_{Si}-(ay_i+bz_i+c)]^2$, where n is the number of strain gages in the cross section. Coefficients a, b, c were obtained imposing $dE/da=0$, $dE/db=0$ and $dE/dc=0$. It is worth noting that when the plane approximation is applied, the strains used for computing the energy dissipated by the steel at points where data provided by gauges are available, are not the actual strains provided by the gauges, but

the strains estimated with the plane approximation. The degradation of anchorage conditions of the longitudinal reinforcement under cyclic loading is not necessarily the same in all rebars of the section; this can cause significant differences in rebars strains due to different bond degradation that are not captured with the plane approximation.

b) *Surface approximation.* The function "scattered interpolant" implemented in the software MATLAB [6] was used to determine the strain at each fiber and time step. Inside the perimeter defined by the rebars instrumented with strain gages the interpolation is done with a function with continuity type C1 [7]. Outside this perimeter the extrapolation is done using the gradient calculated in the perimeter [6]. It is worth noting that when the surface approximation is used, the strains used for computing the energy dissipated by the steel at points where data provided by gauges are available are always the actual strains provided by the gauges. That is, the surface passes through the points where the actual strain is measured during the test. This means that if all rebars of the section are instrumented with gauges, the energy dissipated by the steel with the surface approximation is "exact". In this case, the possible differences in rebars strains due to different bond degradation are captured.

Figure 6 shows an example for each approach. While rebars remained in the elastic range, the surface obtained with both approaches was very similar. However, notorious differences among both approaches can be found when rebars undergoes plastic deformations, as seen in the figure.

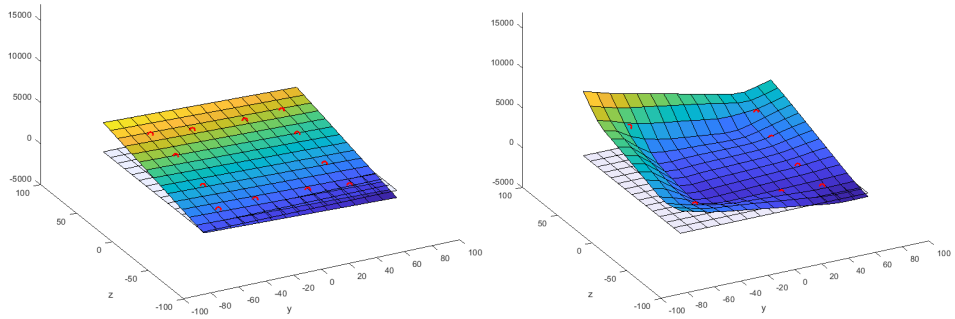

Figure 6: Cross section deformation. Approximation with plane (left) and with surface (right)

Once the strains of the $N \times N$ fibers of the section were determined the corresponding stresses were estimated as follows. The stress on steel fibers $\sigma_{Sr}(t)$ were estimated using an energy conservative steel constitutive model (the Menegotto-Pinto model) [8]. The model incorporates strain-hardening and Bauschinger effects. Figure 7 shows the stress-strain curve obtained for this constitutive model and a loading history consisting of cycles of incremental amplitude.

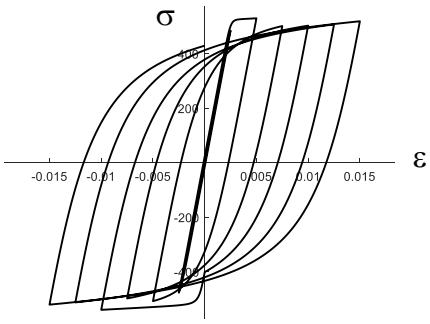

Figure 7: Constitutive law used for steel

The stress on concrete fibers $\sigma_{Cr}(t)$ were estimated using four different constitutive models proposed in the literature and referred to hereafter as C01, C02, C07 and M. The stress vs strain plot for each model are shown in Figure 8. Models C01 and C02 were developed by Mohd [9] and model M is a simplified version of the model developed by Maekawa [10]. As can be observed in the figure, the main difference between model C01 and the other two models (C02 and M) is the shape of the unloading and reloading branches. In model C01 the unloading and reloading branches follow the same path, hence no energy is dissipated when reloading. In models C02 and M unloading and reloading branches follow different paths and some amount of energy is dissipated when reloading. Model C07 is the well known Mander model [11] and differs with the other three models in the shape of stress-strain curve when the concrete is reloaded after having experienced some permanent deformations in previous cycles. The simplification made in the Maekawa model consisted on neglecting the resistance of the concrete in tension and the re-contact effect. The common mechanical properties adopted for concrete in all models are: Young`s modulus E_c=30000 MPa, compressive strength f_c=43 MPa, strain at maximum compressive stress 0.28%. The four models were calibrated so that the area enclosed by the stress-stain curve under monotonic loading was the same. This was attained modifying slightly the strain at failure, that resulted in all cases very close to 1.5%.

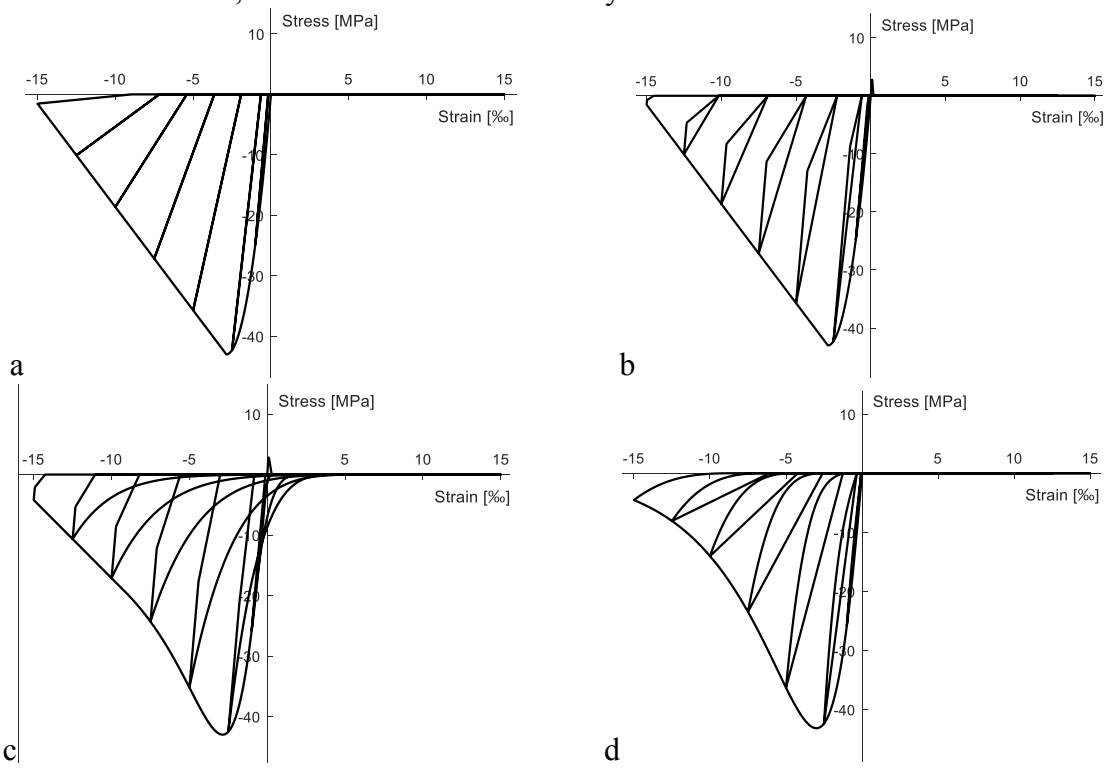

Figure 8: Constitutive laws used for concrete: a) C01; b) C02; c) C07; d) Maekawa

Once the stress in each steel fiber and at each instant t of a given plastic hinge k is obtained, the energy dissipated by the steel reinforcement up to this instant, $W_{S,k}(t)$ is calculated as follows:

$$W_{S,k}(t\ \ ) = \sum_{r=1}^{R} \int_{\varepsilon_{sr}(0)}^{\varepsilon_{sr}(t\ \ )} l_p A_{sr} \sigma_{sr} d\varepsilon_{sr} \quad (1)$$

where A_{Sr} the area of rebar r and R is the number of longitudinal rebars in the plastic hinge. Similarly, once the stress in each concrete fiber $\sigma_{Cr}(t)$ is determined, the energy dissipated by concrete $W_{C,k}$ until a given instant t is obtained as follows:

$$W_{C,k}(t\ \ ) = \sum_{concrete\ fibers} \int_{\varepsilon_{Cr}(0)}^{\varepsilon_{Cr}(t\ \ )} l_p \frac{b}{N}\frac{h}{N} \sigma_{Cr} d\varepsilon_{Cr} \quad (8)$$

where the summation extends to all concrete fibers of the cross section. The total amount of energy stored and dissipated by a plastic hinge k, W_k, is then:

$$W_k = W_{es,k} + W_{p,k} = W_{S,k} + W_{C,k} \quad (9)$$

Figure 9 shows a typical history of W_k. The recoverable elastic strain energy stored in the plastic hinge, $W_{es,k}$, causes the oscillating part of the t-W_k curve. This part can be easily removed by taking the minimum envelope of the history of W_k. The resulting curve is shown in Figure 9 with bold lines and represents the total dissipated energy W_{pk}.

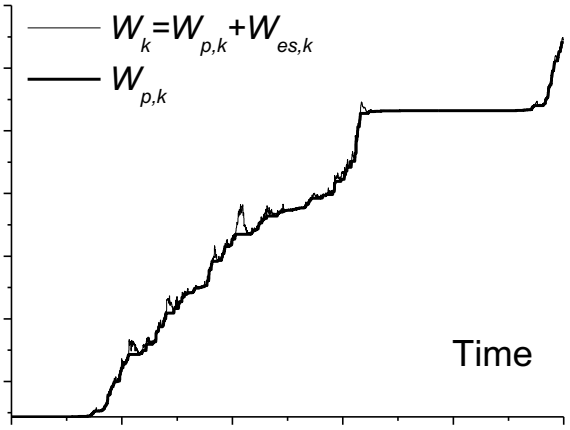

Figure 9: Calculation of W_{pk} from W_k

3.3 Energy dissipated at column bases of BS1 applying different approaches

Influence of plane or surface approximation

Figure 10 compares the total energy dissipated W_{pk} at column C1 base depending on the approximation used to estimate the deformation of the cross section. The comparison is made for the four constitutive laws for concrete (C01, C02, C07 and M) investigated. The abscissa indicates the time measured from the onset of the first test until the end of last test. The intervals of time between tests are not included. It can be seen that: (i) both approximations provide similar results irrespective of the constitutive law used, and (ii) the differences between the plane approximation and the surface approximation tend to be larger as the level of damage increases and the number of cycles of imposed deformations is larger (i.e. with time).

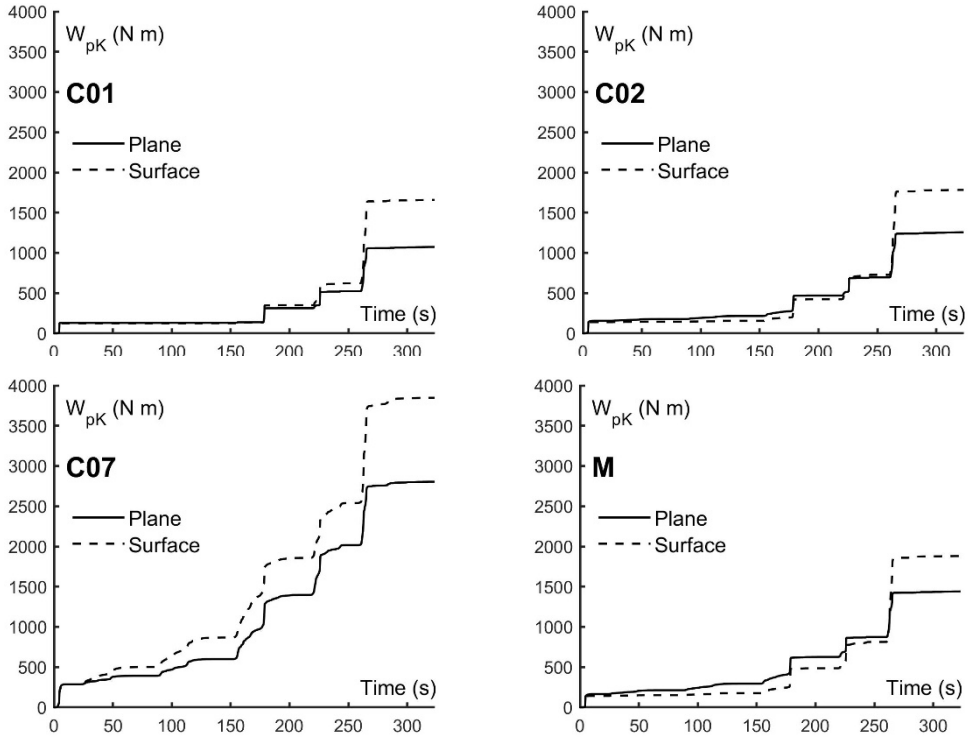

Figure 10: Total dissipated energy in columns using as constitutive law for concrete model: (top left) C01; (top rigth) C02; (bottom left) C07; (bottom rigth) M.

Influence of constitutive law for concrete

Figure 11 compares the total energy dissipated W_{pk} at of column C1 base for the different constitutive laws considered for concrete. The comparison is made for both approaches (plan and surface) used to estimate the deformation of the cross section. As can be seen, constitutive models C01, C02 and M provide similar results; while model C07 estimates a much higher amount of dissipated energy. The reason can be easily found in the shape of the hysteretic loops of each model shown in Figure 8. The area enclosed by the reloading branch up to the stress reached in previous cycle of loading, when unloading in previous cycle reached positive strains is notably higher in model C07 than in models C01, C02 and M. For the columns tested in this study, the use of the constitutive model C07, either using the deformation of the cross section obtained with a plane or with a surface, is not appropriate because it would lead to absurd results as explained next. From measurements provided by the instrumentation during the test, it is possible to estimate the total energy input in the specimen E_I, the energy dissipated by damping W_ξ and the kinetic energy W_k. A detailed calculation can be found in [5]. Figure 12 shows the histories of E_I and $W_\xi+W_k$. The difference $E_I-(W_\xi+W_k)$ must equal to the energy stored/dissipated by the structure (including columns and plate). However, the sum of $(W_\xi+W_k)$ and the energy stored/dissipated by columns estimated with the constitutive law C07 and the plane approximation, curve named $(W_\xi+W_k)+W_{col,plane}$ in Figure 12, or with the surface approximation,

curve named $(W_\xi+W_k)+W_{col,surface}$ in Figure 12, would yield values of total energy that exceed the total input energy, that is meaningless.

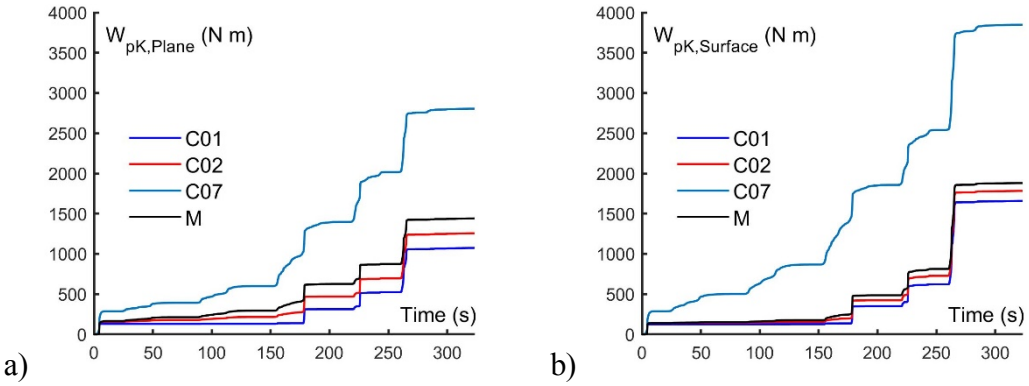

a) b)

Figure 11: Total energy dissipated at base of column C1 approximating the deformation of the section with a: (a) plane; or a (b) surface

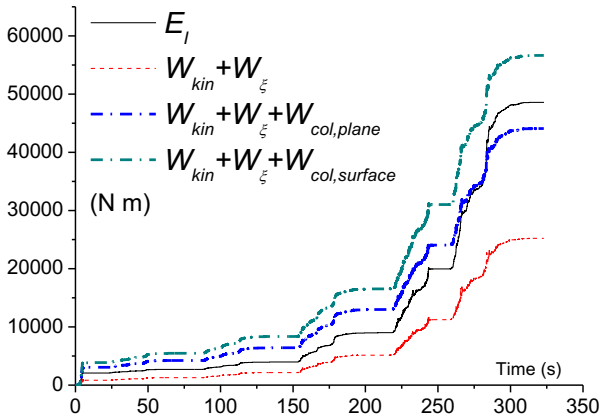

Figure 12: Histories of energy in specimen BS1

3.4 Energy dissipated at base of column C1 under uni- and bidirectional loading

This section compares the energies dissipated by the plastic hinge *k* located at the base of column C1 in specimens BS and BS1. The energies were estimated with the surface approach and the Maekawa constitutive law for concrete described above. Figure 13 shows the energy dissipated by the longitudinal reinforcement, W_{Sk}, by the concrete W_{Sk}, and the total dissipated energy at the plastic hinge, W_k. It is worth recalling that the plastic hinged exhausted its energy dissipation capacity at the end of the test. Therefore, the ordinate of the final point of the W_k curve represents the ultimate energy dissipation capacity of the plastic hinge under unidirectional shaking (left plot of figure 13), and under bidirectional shaking (right plot of Figure 13). It is worth noting that, even though the distribution of dissipated energy between steel and concrete and the history of energies are different, the total amount of energy dissipated up to failure under unidirectional and bidirectional loading are quite similar (2083 Nm for BS and 1879 Nm for BS1); the difference is less than 10%. In other words, these results suggest that the ultimate

energy dissipation capacity of the column is basically the same if the column is subjected to one or to two simultaneous components of the ground motion up to failure.

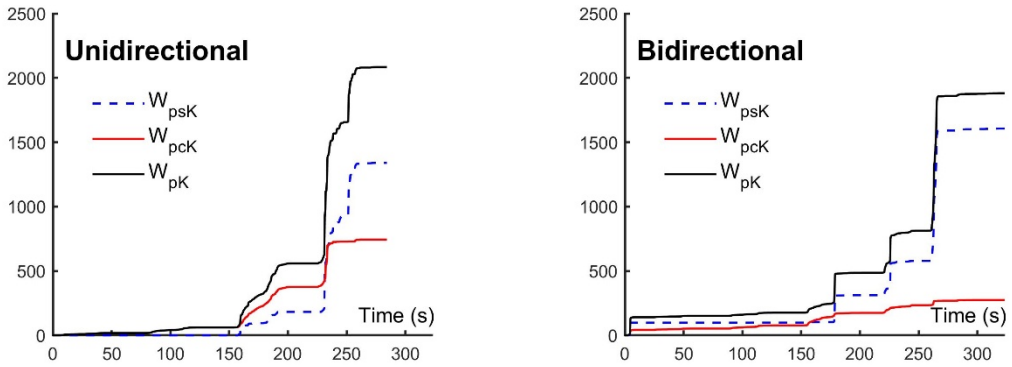

Figure 13: Energy dissipated at the base of column C1 in specimen (left) BS and (right) BS1

3.5 Moment-rotation and axial force-displacement curve at base of column C1 in BS1

For convenience in the following discussion, three axes are defined in the cross section: axis X is perpendicular to the cross section and passes through the centroid; perpendicular axes Y and Z are contained in the cross section and pass through its centroid. When the deformation of the cross section is approximated with a plane, the strain ε in a fiber of coordinates (s_y,s_z) relates to the curvatures ϕ_Y and ϕ_Z and to strain ε_X of the center of gravity by the following expression:

$$\varepsilon = \varepsilon_x + \phi_y s_y - \phi_z s_z \tag{10}$$

The increment of axial force ΔN and bending moments ΔM_Y and ΔM_Z are related to the increments of stress $\Delta\sigma$ and strain $\Delta\varepsilon$ in each fiber by the following equations:

$$\Delta N = \int \frac{\Delta\sigma}{\Delta\varepsilon}\left(\Delta\varepsilon_x - s_z\Delta\phi_z + s_y\Delta\phi_y\right) dA \tag{11}$$

$$\Delta M_y = \int \frac{\Delta\sigma}{\Delta\varepsilon}\left(\Delta\varepsilon_x - s_z\Delta\phi_z + s_y\Delta\phi_y\right)s_y\, dA \tag{12}$$

$$\Delta M_z = \int \frac{\Delta\sigma}{\Delta\varepsilon}\left(\Delta\varepsilon_x - s_z\Delta\phi_z + s_y\Delta\phi_y\right)s_z\, dA \tag{13}$$

Where dA represents the area of the fiber. If the cross section is divided in a discrete number of fibers, the integral symbol is replaced by a sum, and the moment-curvature and axial force-strain relationships can be obtained with an incremental analysis that is summarized in Figure 13.

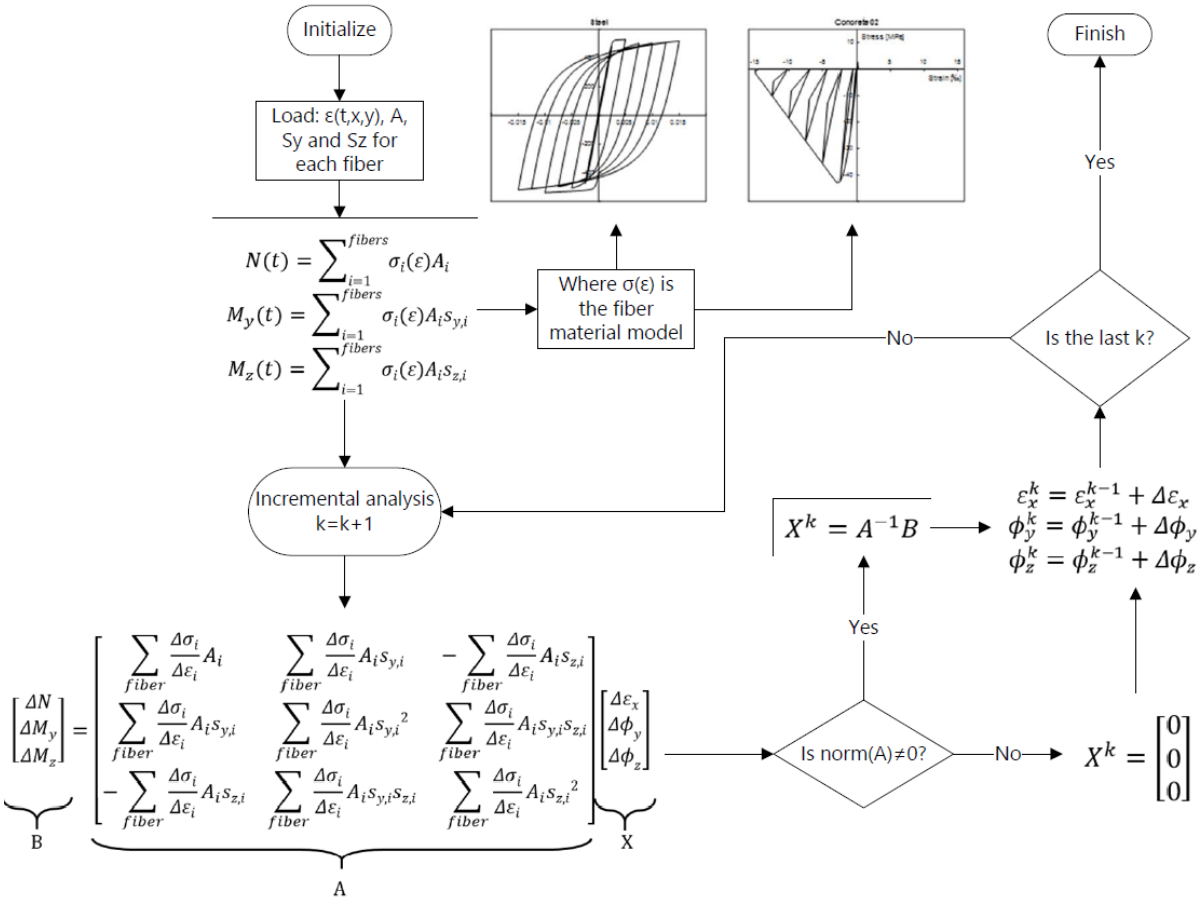

Figure 13: Incremental procedure to obtain the M-ϕ and N-ε of the cross section

Recalling that it has been assumed that the strain in each fiber remains constant along a length l_p (length of the plastic hinge), multiplying ϕ_Y, ϕ_Z and ε_X by l_p provides the rotations θ_Y, θ_Z between the two outermost cross sections of the plastic hinge, and the elongation of the central fiber of the plastic hinge. Figure 14 shows the N-Δ, M_Y-ϕ_Y and M_Z-ϕ_Z relationships obtained for the base of column C1 in specimen BS1, using the plane approximation and the constitutive law M.

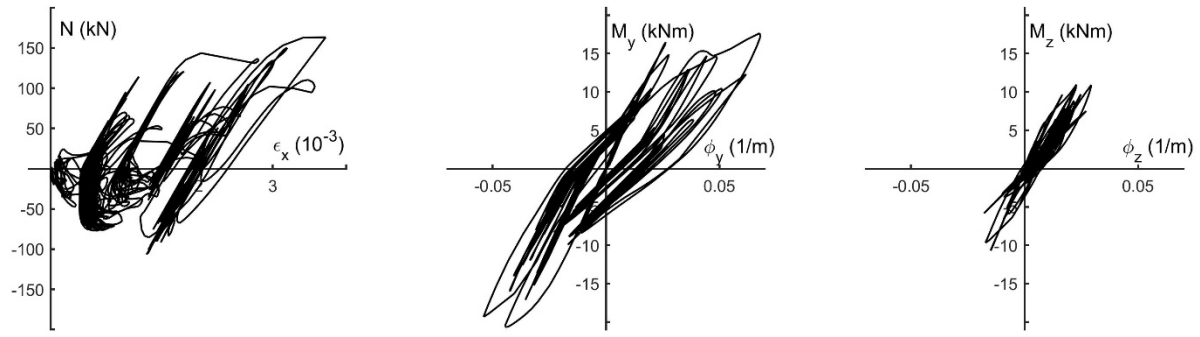

Figure 14: Moment-curvature and axial force-axial strain curves

4 CONCLUSIONS

The energy dissipated until failure at the base of two identical RC columns is investigated experimentally through shake table tests. The columns were tested within two partial structures (specimens) consisting of RC waffle flat plate systems. One specimen was subjected to one horizontal component of the ground motion, and the other specimen to two horizontal components. The energy dissipated by the columns was estimated from the readings provided the strain gauges attached to the longitudinal reinforcement by applying two approaches for estimating the deformation of the cross section (plane approximation and surface approximation), and using four different constitutive laws for concrete. The main conclusions can be summarized as follows:

1. The plane and the surface approximations provide similar results (irrespective of the constitutive law used for concrete) for low levels of damage (i.e. low number of cycles of imposed deformations on the plastic hinge). However, as the level of damage increases the differences become significant. One possible explanation if that the surface approximation can capture differences in steel strains due to different degrees of degradation of the anchorage conditions of the rebars under a large number of cyclic reversals. The plane approximation cannot capture these effects.
2. For the columns tested, the constitutive laws developed by Mohd and implemented in Opensees as concrete type C01 and C02, and the model developed by Maekawa provide similar results (i.e. similar values of the energy dissipated by concrete). However the model developed by Mander and implemented in Opensees as concrete type C07 is not appropriate for the particular column tested because it yields amounts of dissipated energy that exceed the total energy input during the tests to the overall specimens.
3. The ultimate energy dissipation capacity of the column is basically the same if the column is subjected to one or to two simultaneous components of the ground motion up to failure.

ACKNOWLEDGEMENTS

This work is partially funded by the European Union under the program H2020 with the project SERA “Seismology and Earthquake Engineering Research Infrastructure Alliance for Europe”, responding to the priorities identified in the call INFRAIA-01-2016-2017 Research Infrastructure for Earthquake Hazard H2020-INFRAIA-2016-1.

REFERENCES

[1] M. Fardis, From force- to displacement-based seismic design of concrete structures and beyond. *16th European Conference on Earthquake Engineering*, Tessaloniki, Greece, 2018.

[2] H. Akiyama, Earthquake-Resistant Limit-State Design for Buildings. University of Tokyo Press, Tokyo, Japan, 1985.

[3] A. Benavent-Climent, An energy-based damage model for seismic response of steel structures. Earthquake Engng Struct. Dyn. 2007; 36:1049–1064.

[4] A. Benavent-Climent, J. Donaire-Avila, E. Oliver-Saiz, Shaking table tests of a reinforced concrete waffle–flat plate structure designed following modern codes: seismic performance and damage evaluation. *Earthquake Engng Struct. Dyn.*; **45**:315–336, 2016.

[5] A. Benavent-Climent, D. Galé-Lamuela-Jesús Donaire-Avila. Energy capacity and seismic performance of RC waffle-flat plate structures under two components of far-field ground motions: shake table tests. *Earthquake Engng Struct. Dyn.* In press, 2019.

[6] Mathworks, 2018-last update, Matlab and Simulink user's guide. Available: https://es.mathworks.com.

[7] R. Sibson, ‘‘A brief description of natural neighbour interpolation’’ in Interpreting Multivariate Data, V. Barnett Ed., pp. 21–36, Wily, Chichester (1981).

[8] Filippou, F. C., Popov, E. P., Bertero, V. V. (1983). "Effects of Bond Deterioration on Hysteretic Behavior of Reinforced Concrete Joints". Report EERC 83-19, Earthquake Engineering Research Center, University of California, Berkeley.

[9] Mohd Hisham Mohd Yassin, "Nonlinear Analysis of Prestressed Concrete Structures under Monotonic and Cycling Loads", PhD dissertation, University of California, Berkeley, 1994.

[10] Mawkawa, Koichi; Okamura, Hajime; Pimanmas, Amorn. Non-linear mechanics of reinforced concrete. CRC Press, 2014.

[11] Chang, G.A., and Mander, J.B., (1994) "Seismic Energy Based Fatigue Damage Analysis of Bridge Columns: Part 1 – Evaluation of Seismic Capacity," NCEER Technical Report No. NCEER-94-0006 State University of New York, Buffalo, N.Y.